

Remote and In-Situ Irradiance (E) and Aerosol Optical Thickness (AOT) Comparisons

LCDR Joe Martin

September 17, 2004

OC3570-Summer 2004

*Departments of Meteorology and Oceanography, Naval Postgraduate School, Monterey,
California*

1. Introduction

The OC 3570 cruise (Fig 1) on the R/V PT SUR took place from 4-11 August 2004. Leg 1 was from Moss Landing to Port San Luis (4-7 Aug) and the Leg 2 was from Port San Luis to Port Hueneme (7-11 Aug).

The purpose of this project was to do comparisons of irradiance (E) and Aerosol Optical Thickness (AOT) between in-situ (handheld and ship-mounted) and remote (satellite) sensors. This project was the first time a student at the Naval Postgraduate School (NPS) did measurements at sea using handheld Microtops sensors. AOT is an important parameter to be aware of since it is inverse-logarithmically related to visibility, such that higher values of AOT equate to lower visibilities (Fig 2). Since this is the first time this measurement was done, the focus of this project was on data collection and analysis.

Irradiance (or radiant flux density) is “a radiometric term for the rate at which radiant energy in a radiation field is transferred across a unit area of a surface (real or imaginary) in a hemisphere of directions” (AMS Glossary, 2004). It is usually in units of W/m^2 . E is independent of altitude, therefore for a given wavelength or wavelength band, the

amount of E received at the handheld sensors or on the mast mounted sensors should be very similar. Any differences would be due to collection techniques and/or sensor calibration. Since satellites measure radiance, this project compared E between the Microtops and ship-mounted sensors. Figures 3 and 4 show surface irradiance and transmittance spectra respectively.

AOT is “measured vertically above some given altitude and due to extinction by the aerosol component of the atmosphere. AOT typically decrease with increasing wavelength and are much smaller for longwave radiation than for shortwave radiation. Values vary widely depending on atmospheric conditions, but are typically in the range 0.02–0.2 for visible radiation (400-700 nm)” (AMS Glossary, 2004). AOT is a dimensionless parameter. Since AOT is dependent on wavelength and the ship-mounted sensors were all broadband, this project only compared AOT between the Microtops and satellites.

2. Measurements

A. Handheld Sensors

The handheld instruments consisted of two Solar Light Company Microtops II sunphotometers (MT, Fig 5). Each MT has five optical collimators (one for each wavelength, Table 1) and narrow bandpass filters with internal baffles to prevent internal reflections. There is a laser aligned sun target and pointing assembly to ensure best results. The collimators and bandpass filters capture incoming radiation and radiate it onto photodiodes. The radiation is amplified and converted into a digital signal. There are three samples/second during a 10-second scan; therefore, there were 32 samples/scan.

To account for the pitching and rolling of the ship, three successive scans were made on the fantail (height about 2 meters) during each collection period. Hence, the 32 samples/scan were averaged internally and the three scans were averaged in a spreadsheet (Tables 2 and 3). In order to get valid results, collection periods could only occur during cloud-free daylight hours and for *AOT* comparison, periods to coincide with polar orbiting satellites overpasses (Table 4). To avoid extra atmospheric contamination at low sun angles (due to longer paths), the collection periods were primarily done between 1000-1400L (1700-2100Z). This resulted in a maximum of approximately 34 possible collection periods during the cruise (Table 4). A Garmin® GPS 12 Personal Navigator® was connected to one of the MT's for location and time input. Since the scans were done using both MT's simultaneously, the data was transferred to the other MT.

The *E* is calculated by multiplying the signal by a wavelength specific irradiance calibration constant. The result is the *E* per unit wavelength. Integrating by the Full-Width, Half-Maximum (FWHM, Table 1) gives the *E* per wavelength, which was used for comparison to the ship-mounted sensors

AOT calculation assumes Bouguer-Lambert-Beer Law (BLB) which is an empirical relationship relating the absorption of light to the properties of the material the light is traveling through. There is an exponential dependence between the transmission of light through a substance and the concentration of the substance, and between the transmission and the length of material that the light travels through. MT uses the following equation to calculate *AOT*:

$$AOT_{\lambda} = \frac{\ln(V_{0\lambda}) - \ln(V_{\lambda} \times SDCORR)}{M} - \tau_{R\lambda} \times \frac{P}{P_0}$$

where:

$\ln(V_{0\lambda})$ is the AOT calibration constant

V_{λ} is the signal intensity

SDCORR is the Earth-Sun distance correction

M is the optical airmass

$\tau_{R\lambda}$ is the Rayleigh optical thickness

P is the station pressure

P_0 is the standard SLP (1013.25 mb)

AOT calculations of the satellite data were accomplished using a NPS and Naval Research Lab (NRL) algorithm. To summarize, the algorithm first assumes a marine environment aerosol distribution and a single scatter albedo of one. Then a radiance ratio is calculated using AVHRR channels 1 and 2. Using this ratio, the view geometry, and a scattering phase function, a radiance sensed at the satellite can be converted into an *AOT*.

See Durkee (1991), Brown (1997), and Kuciauskas (2002) for more info.

B. Ship-Mounted Sensors

There were two sets of sensors on the PT SUR. One set was mounted on the railing just above the bridge and the second set was mounted on the mast. The heights for the first set were about 8 meters and the second set was at about 15 meters. However, since these sensors were only used for *E* comparisons, the height difference is negligible. The lower set consisted of an Eppley Laboratory Inc. Precision Spectral Pyranometer (PSP), which measures shortwave (SW) radiation in a bandwidth from 280-2800 nm (nanometers) in W/m^2 and an Eppley Precision Infrared Radiometer (PIR), which measures longwave (LW) radiation in a bandwidth from 3500-50000 nm in W/m^2 (EPLAB, 2004). Only the PSP sensor was used for this project. The upper set consisted of the same PSP and PIR sensors as well as a Biospherical Instruments Inc. QSP-2000

Photosynthetically Active Radiation (PAR) sensor. The PAR is another SW radiation sensor, which measures shortwave radiation in a bandwidth from 400-700 nm in $\mu\text{E}/\text{m}^2/\text{s}$ where μE is micro-Einsteins, a unit of illuminance (or light intensity) (Biospherical Inc, 2004).

C. Remote Sensors - Satellites

Polar orbiting satellites were used in this project due to their higher spatial and spectral resolution capabilities. Two National Oceanic and Atmospheric Administration (NOAA) satellites were used, N-16 and N-17, with their Advanced Very High Resolution Radiometer (AVHRR) 1 km spatial resolution sensors. Only Channels 1 and 2 were used since they are the SW channels (NOAA KLM Users Guide, 2004). Table 5 lists the wavelengths used for the various satellites. Two National Aeronautics and Space Administration (NASA) satellites (AQUA and TERRA) were also used (MODIS Info, 2004). The AQUA satellite has the 1 km spatial resolution Moderate Resolution Imaging Spectroradiometer (MODIS) sensor while the TERRA satellite has a MODIS sensor as well as a 1 km spatial resolution Multi-angle Imaging SpectroRadiometer (MISR) sensor. The MISR sensor is unique since it has the capability to look up to 70 degrees forward and aft of nadir. This allows *AOT* calculations in sunglint areas, since it can use other angles besides nadir. See Table 6 for wavelength and angle details (MISR Info, 2004).

3. Analysis

A. Irradiance

The data from the lower set of radiation sensors was provided in an American Standard Code for Information Interchange (ASCII) text file. The data from the upper set

of radiation sensors was provided in a Matrix Laboratory (MATLAB) formatted file. In both cases, a MATLAB script was used to search for, and extract the location, time, and irradiance data corresponding with the MT collection periods. The data was imported into a Microsoft Excel spreadsheet for further analysis (Tables 2 and 3).

Utilizing software included with the MT sensors, the location, time, and irradiance was imported into the same Excel file for comparison to the ship-mounted sensors. Since the MT sensors measure irradiance at discrete very narrow wavelengths and per unit wavelength, each of the values had to be multiplied by the FWHM to first get the total irradiance per wavelength and then summed and the three scans averaged to get a representative “broadband” result to compare to the ship-mounted sensors. The ship-mounted irradiances were also averaged over two minutes since it took about that long to do three MT scans.

There were four problems/issues encountered trying to collect the data with the MT sensors. First, one of the two MT sensors malfunctioned after the cruise so its data was lost. Second, the Sea Level Pressure (SLP) was set to a constant value for each scan. This should have had a minimal affect on E since SLP is not used to calculate E . Third, the motion of the ship resulted in improper aiming of the MT. This would affect the strength of the signal and therefore E . The fourth issue was determining how to convert illuminance units to irradiance units. Biospherical Instruments Inc. (2004) provided a useful Excel spreadsheet to convert different units of energy. The resulting equation to convert $\mu\text{E}/\text{m}^2/\text{s}$ to W/m^2 is as follows:

$$\frac{SPAR}{1.66113 \times 10^{-18}} \times h \times c$$

$$\frac{\lambda}{1 \times 10^9}$$

where:

$SPAR$ is illuminance in $\mu Ein / m^2 / s$

h is Planck's Action Quantum = $6.63 \times 10^{-34} J \cdot s$

c is the speed of light = $3 \times 10^8 m / s$

λ is the wavelength in nanometers (nm)

The irradiance results are discussed in the following section.

B. AOT

The same data processing was done for the MT *AOT* as described above. Satellite data was ordered from NOAA and NASA and was sent to NRL for *AOT* calculations.

The results of the satellite data were entered into an Excel spreadsheet and graphics were created too.

The same three problems/issues were encountered as above. First, data was lost from one MT. Second, the Sea Level Pressure (SLP) was set to a constant value for each scan. Since the formula for *AOT* uses SLP, it could have a greater impact than for *E*. However, during the cruise, SLP had little variation, therefore the impact of this issue was small. Third, the motion of the ship resulted in improper aiming of the MT. This would affect the strength of the signal and optical thickness path more and therefore have a greater affect on *AOT*. Another issue is related to the algorithm. Since the *AOT* values are calculated over a 17 by 17 km area, if over 50 % of the scene is in sunlint, cloud, or land, the algorithm will not produce any values. Results are discussed in the following section.

4. Results

A. Irradiance

As Table 2 shows, the overall result between the MT and the Eppley (low) is the Eppley irradiances are 123.8% increase or 2.24 times the MT irradiances. This result is expected since the range of wavelengths covered by the Eppley sensor is much greater than the MT sensor (335 vs. 2520 nm). Fig 3 shows most of the irradiance is between 300-1000 nm, but there is some additional input from 1000-2800 nm. It is also interesting to note the differences between the two legs of the cruise. On Leg 1, the Eppley showed a 113% increase or 2.13 times over the MT while on Leg 2 the Eppley showed a 146 % increase or 2.46 times over the MT.

The differences between the MT and SPAR were much closer. Table 2 shows the overall result between the MT and the SPAR is the SPAR irradiances show a 5.97% increase over the MT irradiances. This closer result is expected since the range of wavelengths covered by the SPAR sensor is much closer to the MT sensor (335 vs. 300 nm). Figures 3 and 4 show the range of the MT and SPAR sensors is much closer. Again, Leg 1 values are better than Leg 2 values. Leg 1 SPAR values show a 1.5% increase over MT values, while Leg 2 values show a 15.4% increase over MT values.

Lastly, the values of the two Eppley sensors were very close. Overall, they were within 0.5% of each other, which is well within calibration differences. Again, since irradiance is independent of height and they are the same sensors mounted at different heights, provided they are calibrated, the irradiance numbers should be very similar.

B. AOT

Table 3 shows wide variation in *AOT* values between the MT and satellites. There were three valid passes on 05 August and one pass on 06 August. Due to sunglint and cloud/land proximity, there were no valid passes on 10 August. It is also worth noting that the N-16 AVHRR was listed in a “yellow” status since January 2004 (POES Status, 2004). This degradation was due the scan motor current surges. The affect of this condition was not obvious in the data used in the project, but according to NOAA, some images may have artifacts on the edges or within the image itself. The MT *AOT* values were always lower than the satellite values. Excluding one N-16 value that was a 95.6% increase over the MT value (possibly bad data due to scan motor problems), the satellite values showed a 25-32% increase over the MT values. There was also an opportunity to compare MISR to N-17 *AOT* values. In the one case, the N-17 values showed a 44.2% increase over the MISR values. See Figures 6-11 for graphics.

5. Conclusions

A. Irradiance

Some of the differences are likely attributed to the skill in aiming the MT. Excessive motion resulted in errors up to 6 % less irradiance. Other causes could be a high thin cirrus layer contamination or increased aerosols on Leg 2. In addition, during this period, a large fire was burning starting on 08August near San Jose and the offshore flow was advecting the smoke southward. This smoke may have affected the irradiance readings. The results between the two Eppley sensors show that the sensors have equal calibration. The differences in SLP (up to 0.5%) and motion (up to 6%) are probably low enough to

be neglected as making any real difference in the values. Perhaps the largest impact is the differences between the bandwidths of the sensors. When the bandwidth differences were large (MT vs. Eppley sensors), so were the irradiance values. When the bandwidth differences were small (MT vs. SPAR sensor), the irradiance values were much closer. Therefore, unless there is interest in a particular wavelength, the broadband sensors appear to provide good numbers for irradiance. The MT's are more useful for their *AOT* calculations.

B. AOT

For this project, the low *AOT* values correlated with the unrestricted visibility at the times of the MT collects. The aiming skill differences in *AOT* are much more substantial than for *E*. While the motion only affected *E* by up to 6%, *AOT* was affected from 18.3% for minor motion to 39.9% for major motion. The motion caused the *AOT* values to be higher than they actually were resulting in a “worse case scenario”. However, these higher values were still low overall. The SLP error affected the values slightly more than for *E*, but at a maximum of 1.4 %, are probably low enough to neglect. If the SLP pressure varies greatly, this error could have more of an impact. Measurement comparison to satellites is difficult since polar orbiting satellites have poor temporal resolution and even using geostationary satellites (which have better temporal resolution), the algorithm has poor spatial resolution of 17 by 17 km.

Provided the aiming is accurate, the MT *AOT* values are probably better than the satellites since the MT is much higher spatial resolution. In comparing N-17 and MISR, the MISR values are better due to its ability to use more than one angle.

6. Recommendations

The broadband irradiance sensors did a good job of measuring the radiation. The MT sensor is sensitive to motion but not enough to preclude its use aboard a ship. Operator skill would definitely improve the numbers as would a more stable measuring platform (either a larger ship or a gimbaled platform). *AOT* measurements were even more sensitive to motion, but ~~er~~oring on the high side is better than on the low side. Again, operator skill in aiming the MT is key.

Future projects could include trying to calculate *AOT* for the broadband sensors, which would be very involved. Another project could be doing target discrimination based on *AOT* or relating visibilities to *AOT*.

7. References

Brown, B. B., 1997: Remote measurement of aerosol optical properties using the NOAA POES AVHRR and GOES Imager during TARFOX. M.S. Thesis, Naval Postgraduate School, Monterey, CA, 73 pp.

Durkee, P. A., F. Pfeil, E. Frost, and R. Shema, 1991: Global analysis of aerosol particle characteristics. *Atmos. Env.*, **25A**, 2457-2471.

“Glossary Of Meteorology”, AMS Glossary, 17 September 2004, <<http://amsglossary.allenpress.com/glossary>>, [20 September 2004].

Kuciauskas, A.P., 2002: Aerosol optical depth analysis with NOAA GOES and POES in the western Atlantic. M.S. Thesis, Naval Postgraduate School, Monterey, CA, 88 pp.

Microtops II Users Guide, 2003: Solar Light Company, Philadelphia, PA.

“MISR Instrument Specifications”, NASA JPL, 17 September 2004,
<<http://www-misr.jpl.nasa.gov/mission/minst.html>>, [20 September 2004].

“MODIS Technical Specifications”, NASA GSFC, 17 September 2004,
<<http://modis.gsfc.nasa.gov/about/specs.html>>, [20 September 2004].

“NOAA KLM Users Guide”, NOAA NCDC, 17 September 2004,
<http://www2.ncdc.noaa.gov/docs/klm/html/d/app-d.htm>>, [20 September 2004].

“PAR Sensors”, Biospherical Instruments Inc, 17 September 2004,
<<http://www.biospherical.com/BSI%20WWW/Products/Aquatic/Single.htm>>, [20
September 2004].

“POES Status”, NOAA OSO, 17 September 2004,
<[http://www.oso.noaa.gov/poesstatus/componentStatusSummary.asp?spacecraft=16&sub
system=1](http://www.oso.noaa.gov/poesstatus/componentStatusSummary.asp?spacecraft=16&subsystem=1)>, [20 September 2004].

“Precision Spectral Pyranometer”, Eppley Laboratory Inc, 17 September 2004,
<<http://www.eppleylab.com/PrdPrecSpectralPyrmttr.htm>>, [20 September 2004].

“Unit Conversion Spreadsheet”, Biospherical Instruments Inc, 17 September 2004,
<<http://www.biospherical.com/BSI%20WWW/Support/FAQs/LightUnitConversion.xls>>,
[20 September 2004].

8. Figures

OC3570, Summer 2004 (Planning)

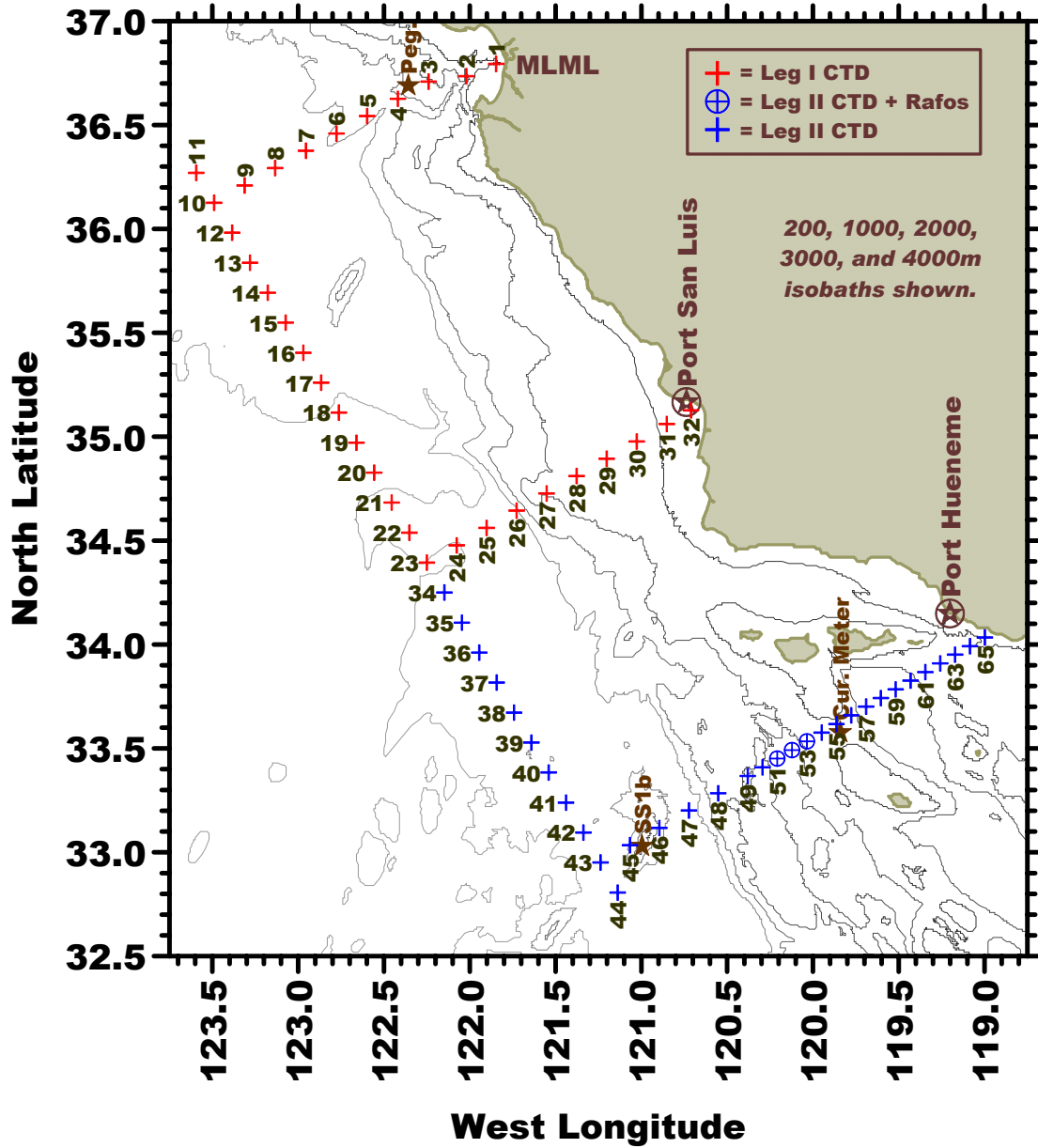


Fig 1

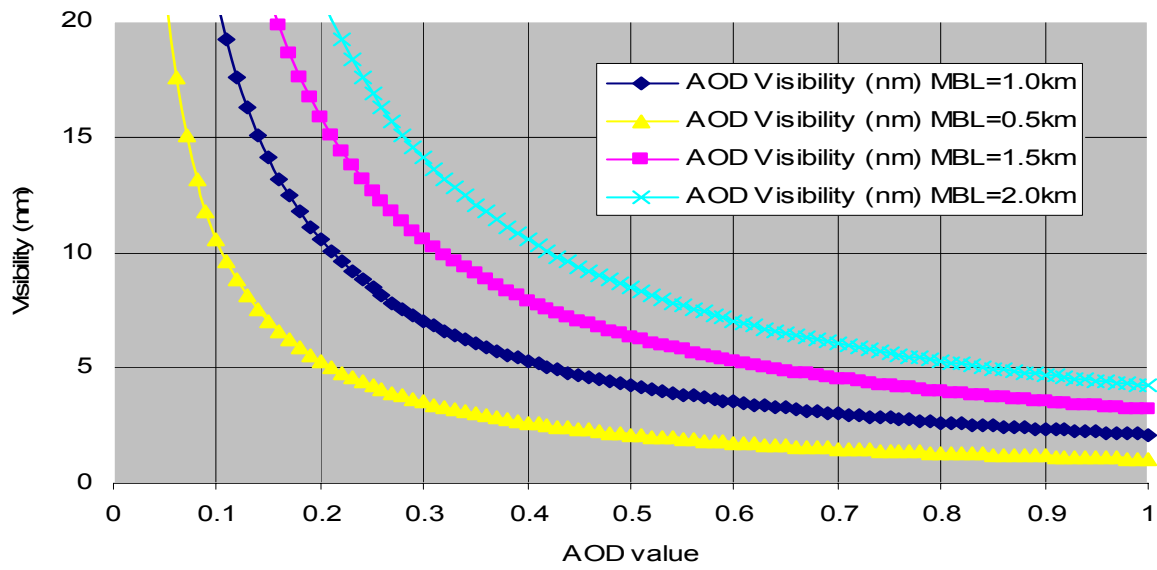


Fig 2

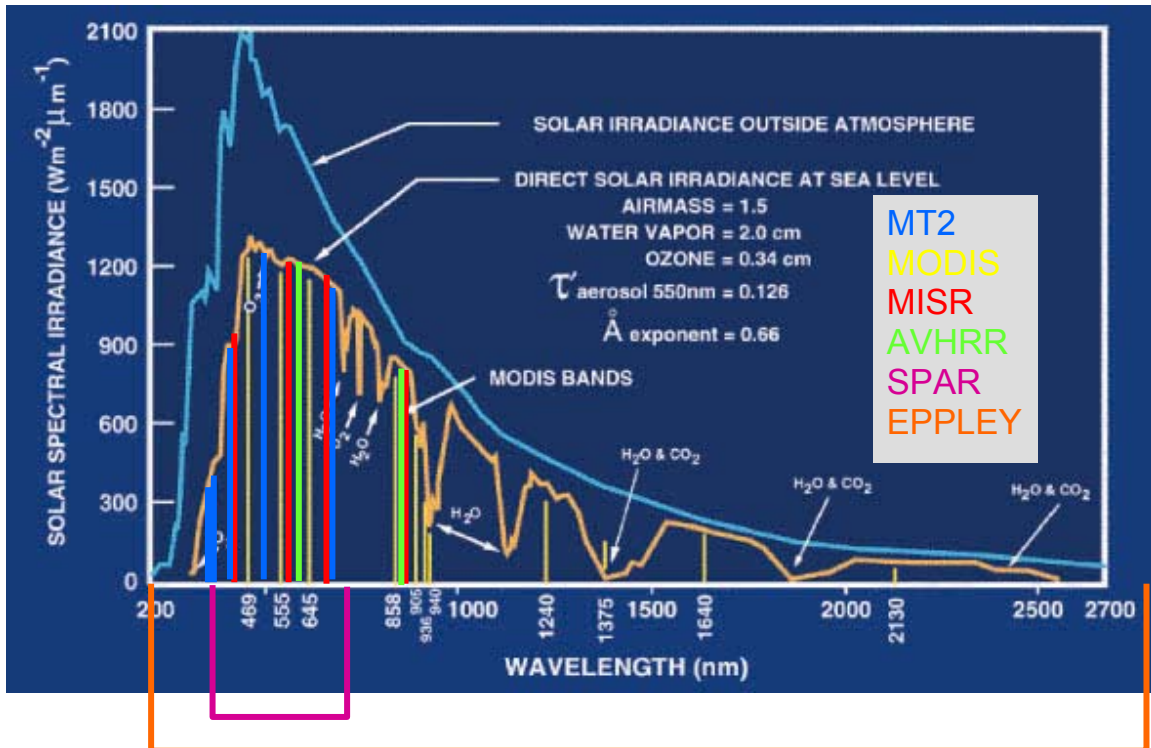


Fig 3

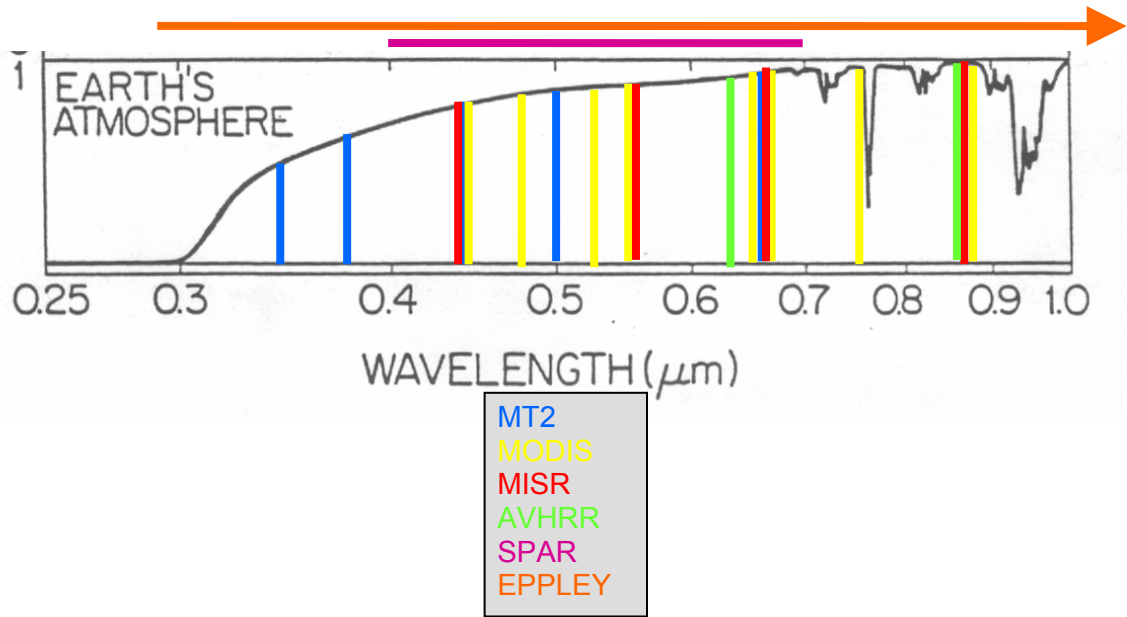


Fig 4



Fig 5

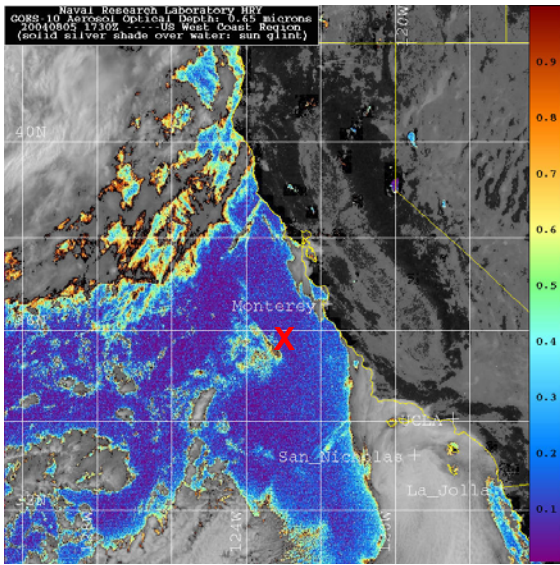


Fig 6

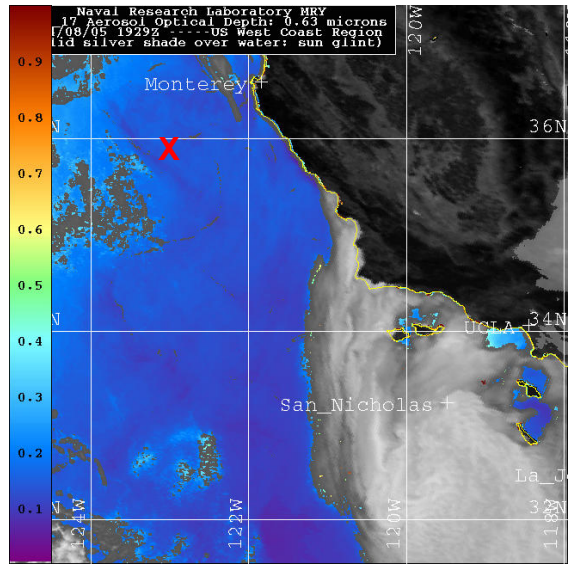


Fig 7

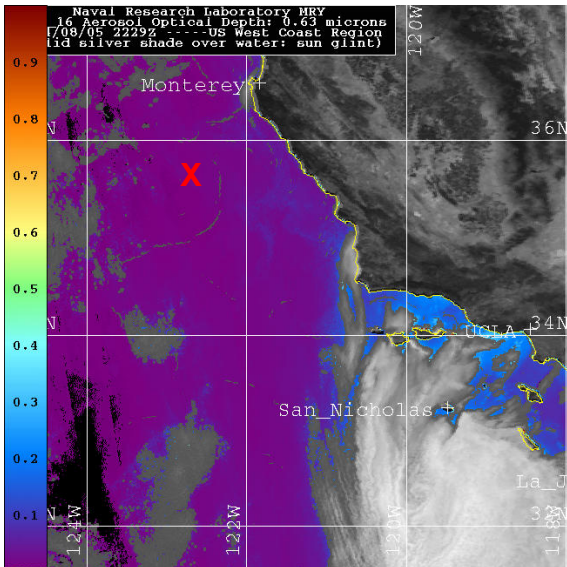


Fig 8

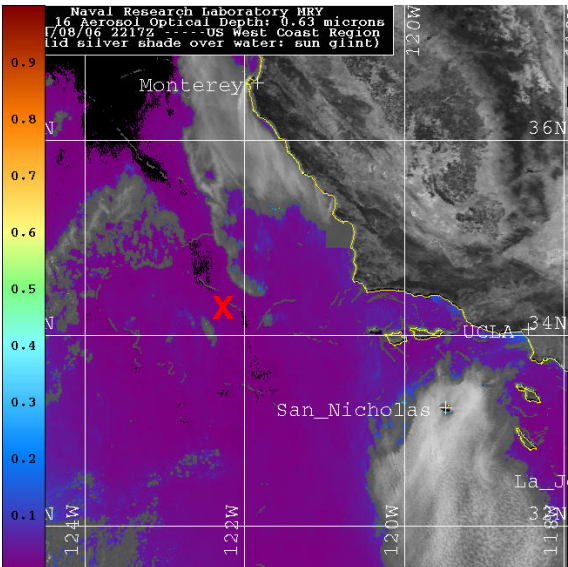


Fig 9

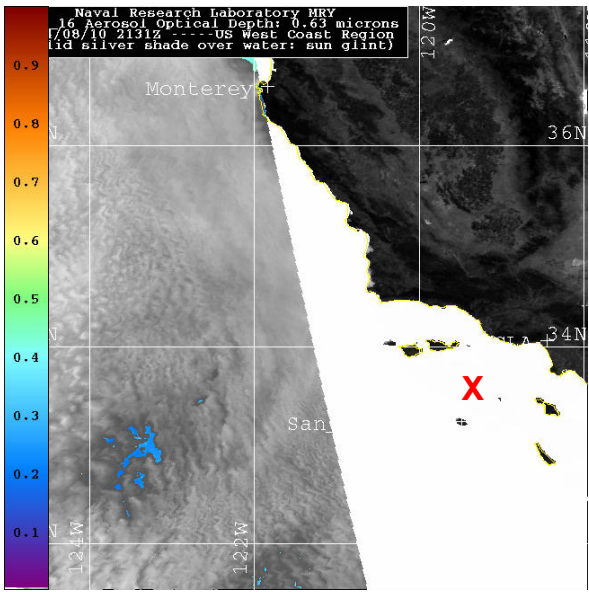


Fig 10

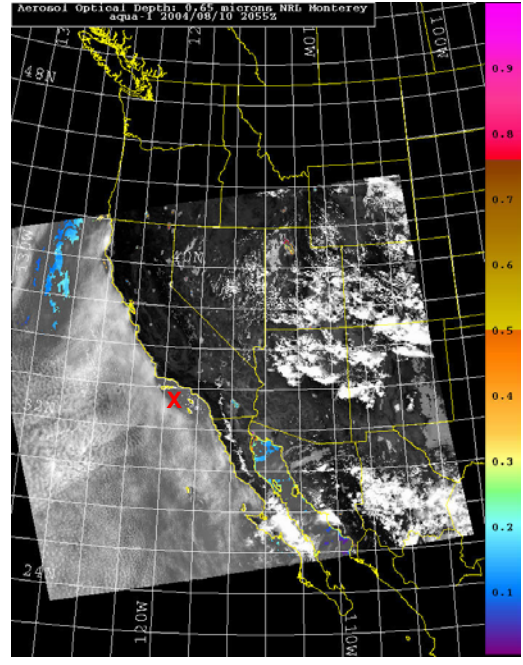


Fig 11

9. Tables

Optical Channels MT #1	Optical Channels MT #2
340 nm (2 FWHM)	500 nm (10 FWHM)
380 nm (4 FWHM)	675 nm (10 FWHM)
440 nm (10 FWHM)	870 nm (10 FWHM)
500 nm (10 FWHM)	936 nm (10 FWHM)
675 nm (10 FWHM)	1020 nm (10 FWHM)

Table 1

N16 and N-17 Channels	Wavelength (nm)	MODIS Channels	Wavelength (nm)
1	630	9	443
2	862	10	488
		11	531
		14	678

Table 5

MISR TYPICAL CAMERA CONFIGURATION

- 275 METERS x 275 METERS (1 x 1)
- 1.1 KILOMETER x 1.1 KILOMETER
- 275 METERS x 1.1 KILOMETER (1 x 4)

CAMERAS:	Df	Cf	Bf	Af	An	Aa	Ba	Ca	Da
ANGLES:	70.5	60.0	45.6	26.1	0.0	26.1	45.6	60.0	70.5
443 nm									
555 nm									
670 nm									
865 nm									

Table 6